Open Access Journal

Journal of Sustainable Research in Engineering Vol. 3 (3) 2016, 63-73

Journal homepage: http://sri.jkuat.ac.ke/ojs/index.php/sri

Mobility Prediction Optimization of Mobile Hosts in Smart Antennas Systems using Adaptive Neuro-Fuzzy Inference System

Nicholas Nkamwesiga [1*], Dominic B. O. Konditi [2] and Heywood A. Ouma [2]

[1]*Department of Electrical Engineering, Pan African University, P. O. Box 62000 - 00200, Nairobi, Kenya*

[2]*Faculty of Telecommunication and Information Engineering, Technical University of Kenya, P. O. Box 52428 - 00200, Nairobi, Kenya*

[3]*Department of Electrical and Information Engineering, University of Nairobi, P. O. Box 30197 - 00100, Nairobi, Kenya*

[*] *Corresponding Author - E-mail: nkamwesiga.nicholas@students.jkuat.ac.ke*

Abstract Owing to the growing demand for wireless communication, the communication network should have better coverage, improved capacity, and higher transmission quality, which contribute to better Quality of Service. The use of smart antenna systems (SASs) is one of the promising technologies in achieving this demand. The SASs achieve this by dynamically radiating shaped signal beams to the mobile terminals in response to received signals. This has the effect of enhancing the performance characteristics such as capacity and hand-over in wireless systems. By using machine learning methods, it is possible to predict upcoming changes in the mobile terminal location at an early stage and then carry out beam forming optimization to alleviate the reduction in network performance. Prediction of Received Signal Strength (RSS) in wireless networks offers a strong base for mobility prediction and localization with minimal effort. The need for mobility prediction is significant and calls for the use of artificial intelligence approaches to make precise and efficient predictions. This paper presents the use of Grey model (GM) which is associated with benefits of reduced overheads in wireless cellular networks and Adaptive Neuro-Fuzzy Inference System (ANFIS) in improving mobility prediction. In this methodology, the ANFIS uses both measured data and the theoretical data used by Log-Normal Shadowing Model (LNSM) to achieve a better estimation of mobility. Mobility is based on the RSS at the mobile node (MN) as it moves towards or away from the transmitting antenna. The approach also takes into account the factors that contribute to the RSS including; path loss exponent, path loss at reference distance and distance of the MN from the transmitter. The results show that ANFIS achieves prediction with a mean absolute error (MAE); between 0.083 m and 0.690 m for short distances (1 m - 65 m), and between 0.322 m and 3.877 m for long distance (100 m - 1800 m). The results were compared against those from other models including the LNSM, GM and generic weighted GM which were found to achieve prediction with larger MAE than ANFIS.

Keywords Adaptive Neuro-Fuzzy Inference System, Grey Prediction Model, Mobility Prediction, Path Loss, Received Signal Strength.

1. Introduction

1.1. Mobility Prediction Problem

There is a high growth rate of mobile and high speed wireless communication networks and mobile users expect to receive excellent quality of service as well as continuous and stable service. The evolution in the capabilities supported by the mobile or wireless networks

is pivotal in achieving the best user experience as reported in [1], [2]. Smart antenna systems (SASs) are expected to provide high-speed data, superior quality voice and location based services. With this motivation, SASs are set to replace the conventional antenna systems and their smartness needs to support real time services for mobile users with minimal signaling delays while enjoying global roaming. Mobile communications technology has evidently developed very rapidly over the past few decades from 2nd to 5th generations (2G-5G) [3]-[5]. To achieve a high data rate, the concept of mobility is considered as a very important feature of wireless networks. Reported studies on mobility and in all the technologies proposed, the mobile node (MN) has a point of attachment to the network known as the access point (AP) or base station (BS), which serves its mobility needs [6]-[8]. When a MN is active in a network, there is a continuous exchange of radio signals between the MN and the BS to which the antennas are attached.

In the investigation of real time monitoring of location and dynamisms in the motion of mobile nodes (MNs) in mobile networks through the use of pilot signal strengths from the serving transmitting stations [9], a model was developed to determine the acceleration of MNs using a dynamic linear system which was supported by regular sampling of the signal strength. The tracking algorithm of this nature is useful in predicting mobility of MNs and thus useful in resource management. The results of the methodology in [9] indicated good accuracy with a large number of parameter values. However, performing prediction of RSS by using raw or preprocessed RSS measurements with an averaging filter would enhance the performance of mobility tracking. Using predicted RSS would yield an estimated value of Received Signal Strength Indicator (RSSI) in cases where a MN is out of range of given BSs or where there is an obstruction that makes it difficult to measure the signal strength accurately [9].

In the area of mobility prediction, an approach based on Grey theory and modelling has attracted attention of researchers because of the benefits associated with it [10]. The Grey model (GM) reduces overheads in wireless cellular networks because it requires little data and thus little processing effort. The GM approach has excellent performance as well as very short calculation time. The processing of the data needs few data points to get a prediction and is therefore suitable for use in real-time systems due to its quick response time [11]-[12].

Mobility prediction has remained an area of active research seeking optimal solutions for tracking and locating MNs in wireless networks. This paper proposes an alternative approach to the reported methods through the use of Adaptive Neuro-Fuzzy Inference System (ANFIS), which is a learning system that aims at reducing the prediction errors and thus make better predictions and contribute to the intelligence of SASs when performing mobility prediction of MNs.

1.2 Log-Normal Shadowing Model

A signal propagation model generates Received Signal Strength (RSS) values. In this research, the log-normal shadowing model (LNSM) is proposed as the target signal propagation model. This is because of its ability to compensate for all the attenuating factors through the use of a Gaussian random variable [13].

In cellular or wireless networks, the location of a MN and its serving base transceiver stations (BTSs) is observable in the information that characterizes the forward link RSS indicator of all the active BTSs. The values of RSSI at the MN are measured and modeled as a two-fold effect of path loss (PL) plus shadow fading [14].

The Path loss, $P_L(d_i)$, at any distance, d_i, in an open space is given in (1) [13].

$$P_L(d_i) = P_L(d_0) + 10nlog_{10}\left(\frac{d_i}{d_0}\right) \quad (1)$$

Where; d_i is the transmitter-receiver separation, n is the power loss (PL) factor, $P_L(d_0)$ is the path loss at known reference distance, d_0. The PL factor is an empirical constant that varies with the characteristics of the propagation environment.

The model in (1) is considered to be ideal and with environmental factors like weather conditions, atmospheric absorption and space rays, the propagating signal is hindered by reflection, diffraction and scattering phenomenon. Based on the empirical evidence, the path loss ($P_L(d_i)$) at any given distance d_i is modeled as a log-normally distributed random variable and is distance-dependent [14]-[17].

The log-normal shadowing model is formed as shown in the following equation.

$$P_L(d_i)[dB] = P_L(d_0)[dB] + 10nlog_{10}\left(\frac{d_i}{d_0}\right) + X_\xi \quad (2)$$

where X_ξ (dB) is a Gaussian random variable.

The RSS at any given distance is modeled by

$$RSSI = P_R = P_T - P_L(d_i) \quad (3.a)$$

$$RSSI = -10nlog_{10}(d) + A \quad (3.b)$$

where; RSSI is the signal power at the MN, P_T denotes the transmitted power, n denotes the path loss exponent, $d = d_i/d_0$ is the normalized distance of the MN away from the transmitter and A denotes the power at d_0. In this

study, d_0 is set between 1 m - 3.5 m for short distance and 100 m for long distance. Both short and long distances are in outdoor environments.

1.3 Grey Prediction Model

Grey forecasting model [18]-[20] is built on Grey theory and has a strong adaptation ability since it requires less data and distribution information is not necessary. It uses minimal data values which are representative of an unknown system in order to formulate a real world problem associated with uncertainty.

The GM(1,1) is a commonly known and widely applied Grey forecasting model [20]. GM(1,1) is a single variable first-order GM. It relies on the original data to reduce the irregularity that exists in the given data set. It is achieved through the following steps:

Step 1: Generate the initial time series as

$$x^{(0)}(t) = x^{(0)}(1), x^{(0)}(2), \dots, x^{(0)}(n), \quad t = 1, 2, .., n \tag{4}$$

where $x^{(0)}(n)$ denotes the n^{th} value of the original sequence.

Step 2: Formulate regular data sequence by applying the Accumulated Generation Operation (AGO) on the initial irregular data sequence in step 1.

$$x^{(1)}(k) = x^{(1)}(1), x^{(1)}(2), \dots, x^{(1)}(n), k = 1, 2, \dots, n \tag{5}$$

where $x^{(1)}(n)$ denotes the n^{th} value of the regular series. The result of the AGO is summarized as

$$x^{(1)}(k) = \sum_{t=1}^{k} x^{(0)}(t) \tag{6}$$

Step 3: Formulate the GM(1,1) differential equation.

The differential equation is formulated as

$$\frac{dx^{(1)}}{dt} + ax^{(1)} = b \tag{7}$$

where; a is the coefficient for reflecting the trends of x^0 and x^1, b is the Grey input. The values of a and b are obtained by applying a least square method to (8).

$$\begin{bmatrix} a \\ b \end{bmatrix} = (B^T B)^{-1}(BY_N)^T \tag{8}$$

where; $B = \begin{bmatrix} -\frac{1}{2}[x^{(1)}(2) + x^{(1)}(1)] & 1 \\ -\frac{1}{2}[x^{(1)}(3) + x^{(1)}(2)] & 1 \\ \vdots & \vdots \\ -\frac{1}{2}[x^{(1)}(n) + x^{(1)}(n-1)] & 1 \end{bmatrix}$ and

$$\boldsymbol{Y}_N = [x^{(0)}(2), x^{(0)}(3), \dots, x^{(0)}(n)]$$

The first column of the B-matrix consists of the background sequence and each point in the sequence forms part of the background value. The values of a and b are obtained by solving (8).

Step 4: Solve the differential equation.

Using the solution of step three (3) and (6), the prediction model in (8) is obtained.

$$x^{(1)}(k+1) = \left[x^{(1)}(0) - \frac{b}{a}\right] e^{-ak} + \frac{b}{a}, k = 1, 2, 3, \dots, n \tag{9}$$

Step 5: Apply inverse AGO.

The Inverse AGO is applied to obtain a prediction value corresponding to the original data series.

$$\hat{x}^{(0)}(k+1) = x^{(1)}(k+1) - x^{(1)}(k) = (1 - e^{-a})\left[x^{(1)}(0) - \frac{b}{a}\right] e^{-ak} \tag{10}$$

Step 6: Validation of the accuracy of prediction.

The accuracy of the GM(1,1) is inspected by testing the accuracy of the prediction and prediction error made by the algorithm. The original data series $x^{(0)}(k) = \{x^{(0)}(1), x^{(0)}(2), \dots, x^{(0)}(n)\}$ and formulated predicted data sequence $\hat{x}^{(0)} = \{\hat{x}^{(0)}(1), \hat{x}^{(0)}(2), \dots, \hat{x}^{(0)}(n)\}$ are used in calculating of residual error, relative error and mean relative error.

The absolute residual error is calculated as shown in (11).

$$\varepsilon_k{}^{(0)} = \left|x^{(0)}(k) - \hat{x}^{(0)}(k)\right|, k = 1, 2, 3, \dots, n \tag{11}$$

The relative error is calculated as shown in (12).

$$\Delta_k = \frac{\varepsilon^{(0)}(k)}{x^{(0)}(k)} = \frac{\left|x^{(0)}(k) - \hat{x}^{(0)}(k)\right|}{x^{(0)}(k)}, \quad k = 1,2,3, \dots, n \tag{12}$$

The mean relative error is calculated as

$$e_k = \overline{\Delta_k} = \frac{1}{n}\sum_{k=1}^{n} \Delta_k \tag{13}$$

The prediction accuracy is given by $(1 - e_k) * 100$ %. When $e_k \leq 0.3$, the GM(1,1) is suitable for medium and long term forecasting [18].

Step 7: Introduce weights in GM(1,1)

Introduce weights, w_1 and w_2, in (4) and (9) to form a new weighted-prediction sequence.

$$\hat{x}_N{}^{(0)}(k+1) = w_1 x^{(0)}(k) + w_2 \hat{x}^{(0)}(k+1)$$

where $\hat{x}_N{}^{(0)}(k+1)$ is the weighted GM, which is a generic prediction based on GM.

1.4 Adaptive Neuro-Fuzzy Inference System

ANFIS uses fuzzy logic and artificial neural networks (ANN). A fuzzy system estimates the output pattern by considering the input patterns which are based on the

membership functions created in the input and output parameters [21]. Neural network (NN) is a mathematical model that is based on the biological neural system [22]. It has interconnected groups of neurons and information is processed based on the connectionist approach to computation.

ANFIS uses FIS at the input layer and learns by tuning input data with an ANN algorithm based on the input-output sets of data presented to it. When a set of input/output data is supplied to the ANFIS, it generates a FIS. The membership function parameters of the FIS are tuned by either a back-propagation algorithm alone or in combination with a least squares type method [22]. The fuzzy systems learn from the adjustments that are made in the membership functions of the data they are modeling [23].

ANFIS structure consists of antecedent and conclusion parts. These two parts are linked by rules, to form a network. During the hybrid learning process, two steps are involved: a feed forward and feedback. In the feed forward, the parameters are first initialized while keeping the antecedent parameters fixed, input data and functional signals propagate forward to compute the result of each layer node and the Least Square algorithm computes the consequent parameters. When the consequent parameters are identified, the functional signals continues in the forward motion until the error measure is computed and therefore known. In the feedback phase, the error rates propagate in a reverse order, from the output towards the input end [22-24]. The process is continued until the number of specified epochs (iterations) have been attained or error reaches a preset threshold.

Fig.1 [25] shows the architecture of an ANFIS. It assumes a system with two inputs (x, y), four rules and one output (z). The ANFIS structure executes the rules and calculates the output through five layers: fuzzification, product, normalization, de-fuzzification and total output. This ANFIS structure has four rules and by using first-order Sugeno model, a typical set of fuzzy if-then rules are generated as

$$If\ x\ is\ A_1\ and\ y\ is\ B_1, then\ Z_1 = p_1x + q_1y + r_1 \quad (14.a)$$

$$If\ x\ is\ A_1\ and\ y\ is\ B_2, then\ Z_2 = p_2x + q_2y + r_2 \quad (14.b)$$

$$If\ x\ is\ A_2\ and\ y\ is\ B_1, then\ Z_3 = p_3x + q_3y + r_3 \quad (14.c)$$

$$If\ x\ is\ A_2\ and\ y\ is\ B_2, then\ Z_4 = p_4x + q_4y + r_4 \quad (14.d)$$

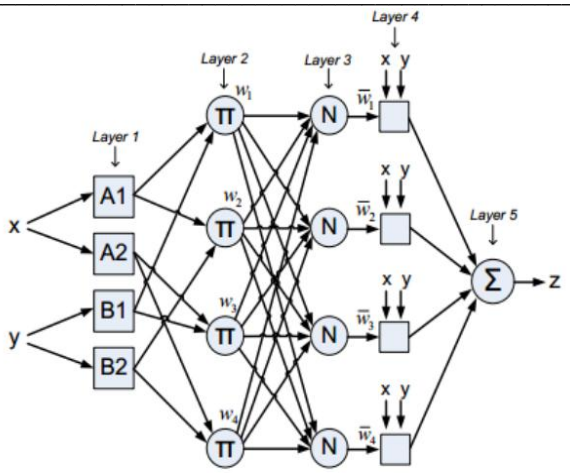

Fig. 1. Structure of an ANFIS

In Fig.1 and (14), A_1, B_1, A_2, B_2 are fuzzy sets, p_i, q_i and r_i $(i = 1,2,3,4)$ are the coefficients of the first order polynomial linear functions.

The different layers in Fig. 1 are as follows:

Layer 1: Fuzzification Layer

In this layer, the membership values are calculated from the membership relationship between input and output functions of layer 1 and they are identified as

$$O_{1,i} = \mu_{A_i}(x), \quad i = 1,2 \quad (15.a)$$

$$O_{1,j} = \mu_{B_j}(y), \quad j = 1,2 \quad (15.b)$$

Where $O_{1,i}$ and $O_{1,j}$ represent the output functions and μ_{A_i} and μ_{B_j} represent the membership functions.

Layer 2: Product Layer

This layer has four nodes and the output, w_j, of each rule has to be computed by means of a fuzzy AND operation. Eq. (16) illustrates this. w_j is the weight of the j^{th} rule and $O_{2,j}$ is the output Layer 2.

$$O_{2,j} = w_j = \mu_{A_i}(x)\,\mu_{B_i}(y), j = 1,2,3,4.\ i = 1,2 \quad (16)$$

Layer 3: Normalized Layer

The purpose of this layer is to normalize the weight function, w_j, obtained from Layer 2 to generate the normalized output $\overline{w}_j$. The output $\overline{w}_j$ is calculated as the ratio of the j^{th} weight to the summation of the all weights. The output is denoted by

$$O_{3,j} = \overline{w}_j = \frac{w_j}{\sum_{i=1}^{4} w_i} \quad (17)$$

Layer 4: De-fuzzification Layer

In this layer, $\overline{w}_j$ multiplies the related output function (linear equations of the consequent part in (17).
The output of this layer is given by (18).

$$O_{4,j} = z_j \bar{w}_j = \bar{w}_j(p_j x + q_j y + r_j) \quad (18)$$

Layers 5: Total Output Layer

This is the final layer with a single node which gives the overall output. The output, given in (19), is the sum of the outputs of the former nodes.

$$O_{4,j} = \sum_{j}^{4} z_j \bar{w}_j \quad (19)$$

The antecedents are tuned during the training process. Other parameters in the ANFIS training process are the coefficients of the output polynomials as seen in (14) and number of rules. The number of rules is defined by the number of inputs and membership functions [26].

A hybrid algorithm constituting error back propagation and gradient descent method was used in this research for ANFIS learning. Throughout the learning process, the premise parameters of Layer 1 and consequent parameters in Layer 4 are tuned for a desired output. Eq. (20) shows the expression for calculation of the root mean square error *(RMSE)*.

$$RMSE = \sqrt{\frac{1}{N}\sum_{i=1}^{N}(d_i - o_i)^2} \quad (20)$$

Where d_i is the desired output, o_i is the ANFIS output for the i^{th} sample from training data and N is the training sample count.

2. Proposed Mobility Prediction Technique

In Fig. 2, the ANFIS simulates the relationship between the input and output data through training and learning processes. The study used secondary data as the training dataset. This data was gathered from [13]-[15], [27], [28] and given in Table I**.** The testing data was generated by the GM. The inputs of GM were RSS values generated by the LNSM. Through its learning, the ANFIS optimized the RSS values indicated by RSS_A.

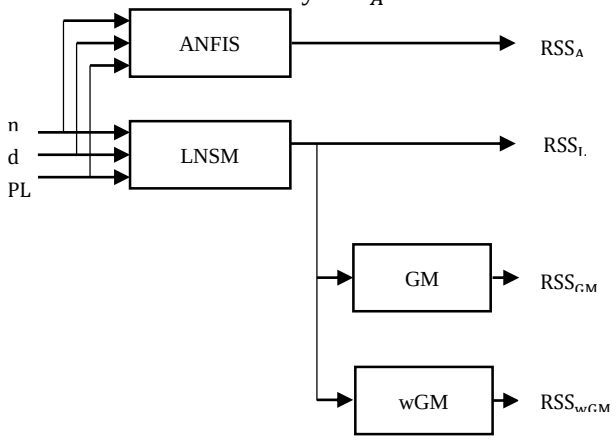

Fig. 2. RSS Prediction Set-up for ANFIS and Other Models

During the simulation process, 106 datasets were used for training and testing. The input data to the ANFIS was the path loss (PL), path loss exponent (n) and distance (d). The output of the system was the optimized RSS values, RSS_A. The input data consisted of set of [4 4 5] membership functions, which generated 80 (4 x 4 x 5) rules. The selection of these membership functions was reached through series of simulations that were performed to check the performance of the system. The performance indicators for the simulation were convergence (or run time) and magnitude of the training error. The selected set of membership function ran for an average time of 120 s with a training error of 0.4016m. The optimized RSS and distance parameters were then used to generate regression models which were used in distance estimations in mobility prediction.

Table 1: Simulation Parameters

b	n	PL_0	d_0	d_m	δ	P_t	Ref
1	1.613	39.00	1.0	61.5	0.4510	0.000	[27]
2	2.200	45.00	1.0	10.0	0.2721	0.000	[15]
3	3.800	47.30	1.0	35.0	0.7270	3.802	[28]
4	3.110	89.77	100.0	1250.0	6.0000	44.771	[14]
5	3.550	106.00	100.0	1800.0	8.0000	0.000	[13]
6	2.570	95.00	100.0	1800.0	5.4000	0.000	[13]

In Table 1, b is an index representing a given dataset, n is the path loss (PL) exponent, $PL_0[dB]$ is the PL at d_0, $d_m[m]$ is the maximum distance covered, $\delta[dB]$ is the standard deviation, $P_t[dBm]$ is the transmission power and Ref denotes the referred and published papers.

3. Simulation, Results and Discussion

All the models used in this research; LNSM, GM and ANFIS were implemented in MATLAB (R2012b). The simulation begun with the LNSM which provided the inputs to the GM as shown in Fig. 2. The Received Signal Strength (RSS_L) is processed by the GM and w-GM to produce outputs; RSS_{GM} and RSS_{wGM}. The (RSS_{GM}) together with input parameters of the LNSM formed the testing data set to the ANFIS. The training data set to the ANFIS was gathered from the published papers [13]-[15], [27]**,** [28]**.**

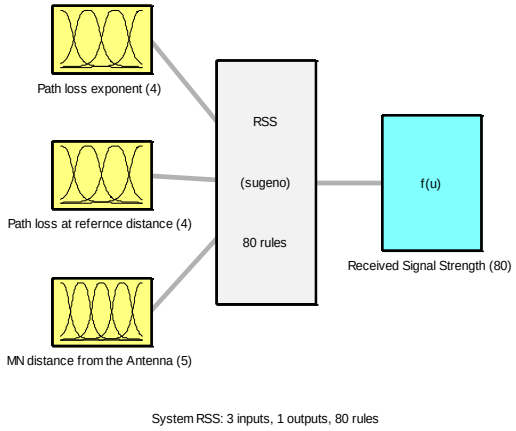

Fig. 3. Proposed ANFIS Model

Fig. 3 shows the relationship between the input and output parameters of the proposed ANFIS model.

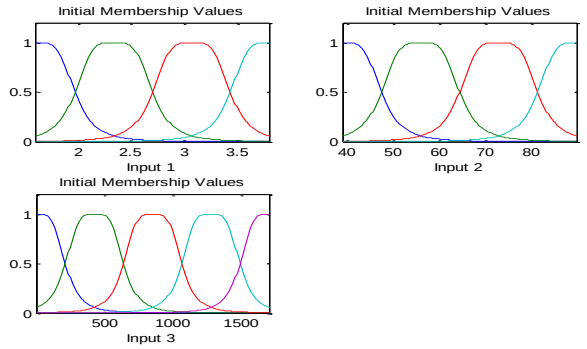

Fig. 4a. Membership of input parameters to the ANFIS model before training

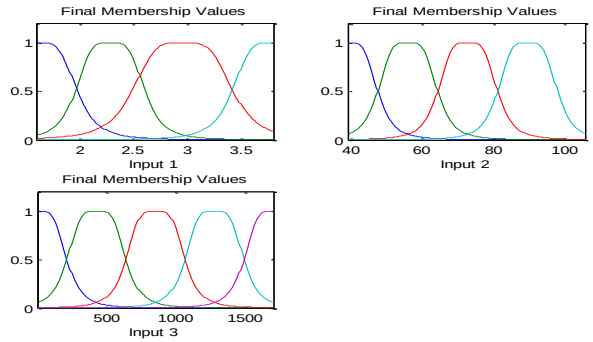

Fig. 4b. Membership of input parameters to the ANFIS model after training

Fig. 4a-b represent the membership values of the input parameters before and after ANFIS training respectively. At the stage of GM prediction, two corrections were made on its output data. The first study involved eliminating the last predicted values as seen in Fig. 5a-b. This involved predicting $(t+1)$ data points, where t is the expected number of data points, and then discarding the one extra point to remain with t points. Using this approach the execution time by 12.83 %. The second study on GM was done to reduce on the error (gap) between the GM and LNSM. This was done by applying weighted averages in the primitive data and the GM predicted data to form the generic version, which is the weighted GM. The weights used in the study were $w_1 = 0.5$ and $w_2 = 0.5$. These values of the weights were chosen at random. After the application of weights, the resulting predicted data has a smaller error than the error existing in GM. This resulted from the application of weighs on original data and the outputs of GM which performed an averaging operation on the two datasets. The impact of the weighted averaging is seen in Fig. 5a-b.

Using (13), the accuracy of GM and weighted GM was investigated. The average accuracy of GM and weighted GM was 96.56 % and 97.86 % respectively. This shows that the prediction accuracy of weighted GM, in reference to the LNSM outputs, is better than that of ordinary GM due to the application of weights in the later.

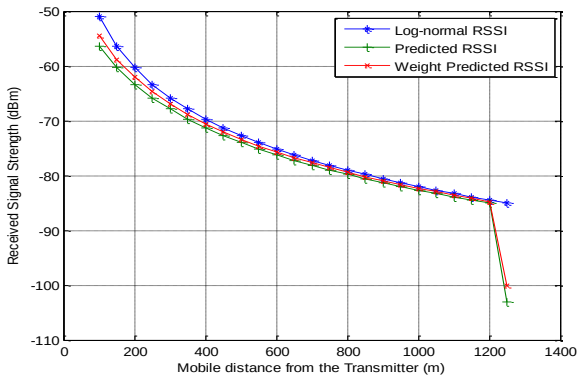

Fig. 5a. RSS versus distance with endpoint error

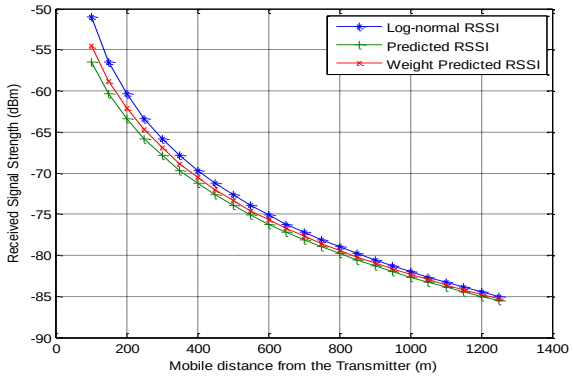

Fig. 5b. RSS versus distance with endpoint error

Three independent studies were performed on ANFIS by subjecting the system to different sets of testing data: the first study involved the use of GM's output; the second one involved the use of LNSM output; and in the last one the wGM outputs were used. Under all these testing data,

the trained outputs of ANFIS exhibited the same behavior with the same results.

Data plots of RSS versus distance are shown in Fig. 6 and 9. In all these plots, five sets of RSS values are plotted against distance. These RSSs values are: measured RSS from published data; optimal RSS, which is the ANFIS output, RSS output from GM; RSS output from the weighted GM; and RSS output from LNSM.

The measured data used in this research consists of data gathered from both long and short distances in outdoor environments. It is evident that the outputs of different predictions follow a similar trend; the RSS at the MN reduces as the distance between the MN and the transmitter increases.

3.1 Short Distance

Fig. 6 shows a plot of RSS versus distance from the transmitter for the four models (ANFIS, LNSM, GM, and wGM) used in this study. Fig.7 shows a plot of localization error against distance for the models indicated in Fig. 6. Fig. 6-8 correspond to index 1 of Table I-II.

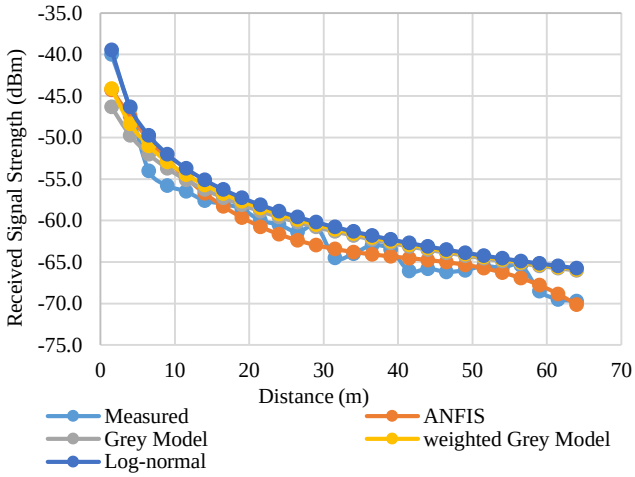

Fig. 6. RSS versus distance for index 1

ANFIS curves in Fig. 6 and 9 form multiple points of intersection with both the training data and testing data with many cross-points being between the ANFIS curves and training data curves compared to the cross-points between ANFIS output curves and the testing data curves. Fig. 6 shows that the measured RSS and ANFIS output values deviate away from their previous general trend at 38 m distance. A similar behavior occurs in Fig. 9 at 1100 m distance.

Table 2: Regression Line Estimations for the Different Prediction Models for Index 1 and 5

b	Regression Line Approximation	R^2
1	$RSS_1(dBm) = -16.746 * log_{10}(d_m) - 40.895$	0.9695
	$RSS_1(dBm) = -16.231 * log_{10}(d_a) - 41.522$	0.9774
	$RSS_1(dBm) = -16.13 * log_{10}(d_l) - 39.451$	1.0000
	$RSS_1(dBm) = -14.081 * log_{10}(d_{wg}) - 42.534$	0.994
	$RSS_1(dBm) = -12.972 * log_{10}(d_g) - 44.315$	0.9881
5	$RSS_6(dBm) = -28.418 * log_{10}(d_m) - 62.36$	0.8809
	$RSS_6(dBm) = -28.367 * log_{10}(d_a) - 62.36$	0.9042
	$RSS_6(dBm) = -35.5 * log_{10}(d_l) - 53$	1.0000
	$RSS_6(dBm) = -30.392 * log_{10}(d_{wg}) - 59.011$	0.9951
	$RSS_6(dBm) = -28.561 * log_{10}(d_g) - 61.56$	0.9935

In Table 2, b is the index; d_m is the ratio d_i/d_0 for the measured data regression line; d_a is the ratio d_i/d_0 for the ANFIS regression line; d_l is the ratio d_i/d_0 for the LNSM regression line; d_{wg} is the ratio d_i/d_0 of the weighted GM regression line; d_g is the ratio d_i/d_0 of the GM regression line; and R^2 is the correlation coefficient (with the actual data) of the estimated regression lines.

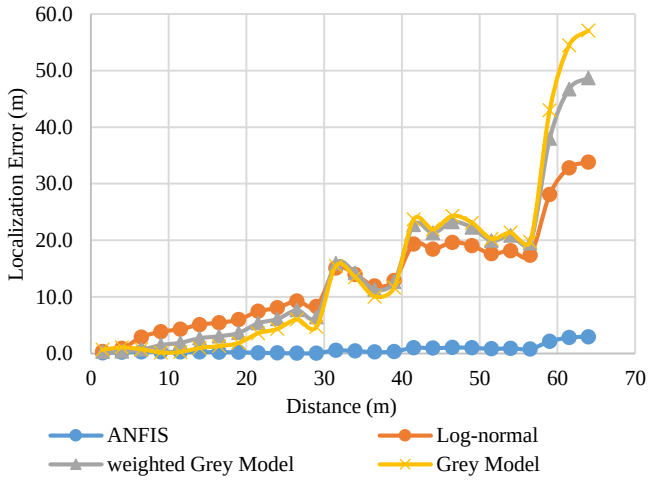

Fig. 7. Localization error for the different prediction models for index 1

From Fig. 7 and 10, it is seen that the mobility prediction is carried out with some errors as the MN moves away from the base station. A large increase in the prediction error in Fig. 7 occurs at 38 m distance. In Fig. 10 this behavior occurs at a distance of 1100 m.

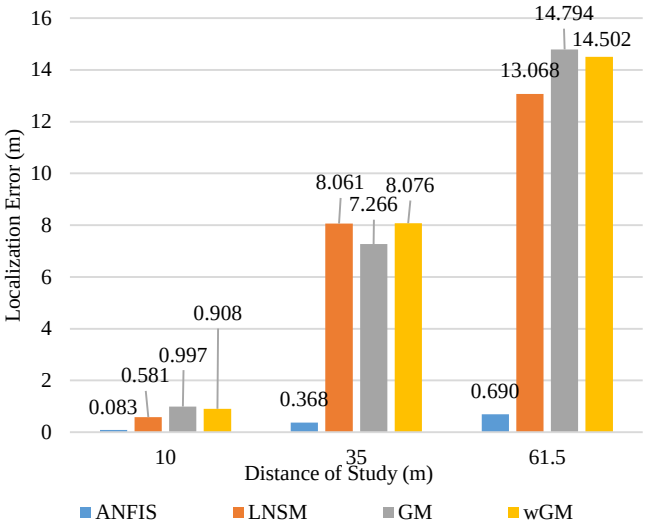

Fig. 8. Comparison of localization error in short distance outdoor environment

3.2 Long Distance

Fig. 9 shows a plot of RSS versus distance for the four models (ANFIS, LNSM, GM, and wGM) used in this study. Fig. 10 shows a plot of localization error against distance for the models indicated in Fig. 9. The Fig. 9-11 correspond to index 5 of Table I-II.

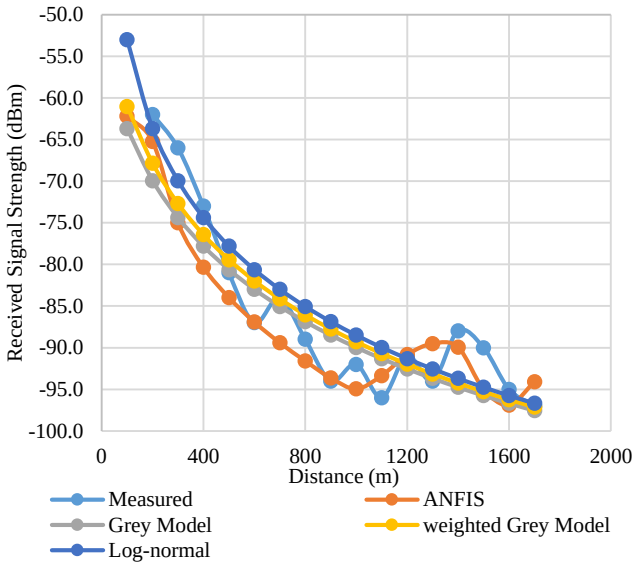

Fig. 9. RSS versus distance for index 5

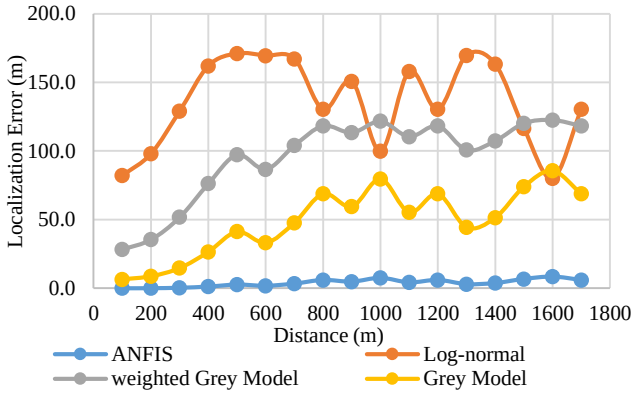

Fig. 10. Localization error for the different prediction models for index 5

The performance of the different prediction models in estimating distance was analyzed by studying the relationship between the RSS values and the logarithmic values of their corresponding distance.

Each figure yielded a set of regression line approximation for the prediction models under the study. These regression lines approximations are summarized in Table II. From Table II, it is evident that the regression line estimates exhibit a general linear equation of a line between two points as shown in (21).

$$y = mx + b \tag{21}$$

Where; $y = RSS$, $m = -10n$, $x = log_{10}(d_i/d_0)$ and b is the intercept on the y-axis. For all the regression line estimates the approximate distance was calculated using (22).

$$d_i = d_0 * 10^{-\left(\frac{RSS+b}{10n}\right)} \tag{22}$$

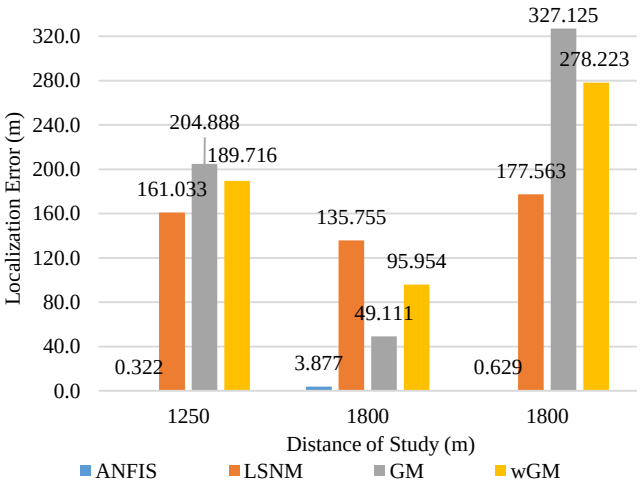

Fig. 11. Comparison of localization error in long distance outdoor environment

All the errors and corresponding root mean square error (RMSE) which are formed by the distance deviations of different predictions from the measured distance using the

results of (22) were computed. These errors are compared as summarized in Fig. 8 and 11 for short and long distance respectively. From these two figures, it is seen that there is a general trend; the mean absolute error (MAE) values increases with increase in distance in both long and short distance communication systems.

Fig. 10 shows that the ANFIS estimates begin to fluctuate at distance of 1100 m. From the distance greater than 1100 m, the error fluctuates with almost a normal distribution around the expected data. The other models like GM and wGM seem to follow the same trend though with different error magnitudes. This behavior is relatively similar to the rest of the datasets under the study under different distances of consideration. The data in this dataset was gathered from a dense urban environment with factories, many offices with communication towers, high dense human and vehicular traffic. All these listed sources of obstructions contribute to a high shadow factor and a poor radio signal reception. The large error at the near end positions is due to the poor learning of ANFIS on the training data.

The data corresponding to index 5 was gathered from an urban environment where as data corresponding to index 4 and 6 was gathered from a suburban environment. For long distance, data gathered from a suburban environment shows that the prediction performance of all models under study is better than the performance of the same models in an urban environment.

For long distances, ANFIS estimates has mean error between 0.322 m and 3.88 m, which values are relatively good for long distance localization of MNs. For short distances, the error in ANFIS is in the range of 0.083 m to 0.690 m. The ANFIS approximates in short distances are good approximations since it is in a fraction of a meter distance.

The estimates made from the LNSM had a large error magnitude. The outputs of their prediction cannot be relied on for real systems. The poor prediction of LNSM are spread to the GM and weighted GM whose inputs are the outputs of the LNSM.

4. Evaluation of Performance

The performance of ANFIS has been evaluated by comparing its localization error, as shown in Fig. 12 and Table III, with other methods and algorithms which are published in [27], [29]-[32].

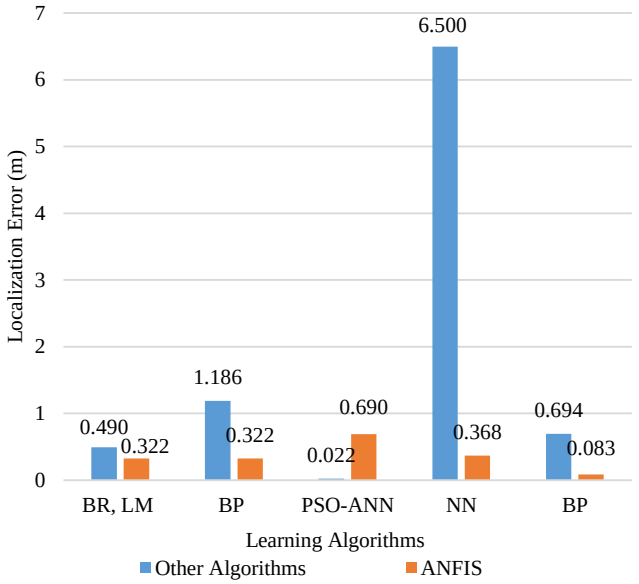

Fig. 12. Comparison of ANFIS errors with other algorithms' errors.

Table 3: Comparison of ANFIS errors with other algorithms' errors.

Other Learning Algorithms			ANFIS	
Algorithms	**Distance (m)**	**Error(m)**	**Distance (m)**	**Error (m)**
BR, LM	300x300	0.49	1250	0.322
BP	100x100	1.186	1250	0.322
PSO-ANN	65	0.022	65	0.690
NN	50x50	6.5	35	0.368
BP	10x10	0.694	10	0.083

In Table 3, a summary of the comparison between ANFIS and other algorithms is presented. BR is the Bayesian Regression, LM is the Levenberg-Marquardt BP is the Back-propagation, PSO-ANN is the Particle Swarm Optimization-Adaptive Neural Network, and NN is the Neural Network. It should be noted that in some cases, different distance measurements were used compared. This was because the models used the same input parameters.

The study shows a superior performance of ANFIS methodology in comparison to the majority of the highlighted algorithms. For short distances, the performance of ANFIS is comparable to that of Hybrid PSO-ANN.

5. Conclusions

The study considered the data gathered from outdoor, short and long distance, environments. The short distance covered 1 m - 10 m, 35 m and 61.5 m whereas the long distance covered 100 m - 1250 m and 1800 m. It was seen that in long distance, data gathered from a suburban

environment contributed to a better prediction performance of all models in comparison with the data gathered from urban environment. Urban environments contains high path loss because of the many obstructions; like storey buildings, vehicles, transmitters, that are present in the path of the radio signals. Generally, prediction error in ANFIS increases with increase in distance between the transmitter and the MN. This is because as distance increases, the sources of radio frequency (RF) signal obstructions increase and the RSS values collected at the MN have rapid variations at those distances. After ANFIS training, the trained output pattern at far distances deviates away from the collected data pattern more than the patterns that are resultant of short distances. It has been discovered that ANFIS prediction methodology performs well up to a given distance as the MN traverses. The average approximated distance at which the anomalies in the accuracy of mobility prediction occurs has been noted as 62.33 % and 64.82 % for short and long distance communication environments respectively. This implies that whenever there is a change in the general trend of ANFIS output values and the measured data, the accuracy in mobility prediction begins to diminish from that point and onwards. During the actual implementation of ANFIS methodology in SASs such points correspond to critical distances and the beam forming characteristics need to be adjusted to counteract the diversion from the normal mobility prediction trend and accuracy.

It is also notable that ANFIS prediction for short distances outperformed its predictions for long distances. This is attributed to the data sampling intervals used in short and long distances; the sampling intervals for short distance was 1 m, 1.5 m and 2.5 m whereas the one for long distance was 50 m and 100 m. Using data gathered from small intervals would yield better approximations in long distances.

This paper has shown how ANFIS may be used to improve mobility prediction. It has been compared with other conventional models; LNSM, GM and wGM and found out to outperform all these models. Evaluation was by comparison with other published methods and results for the same data inputs. The study has revealed that using ANFIS in mobility prediction of MNs yields a better prediction performance than many traditional methods due to its leaning ability.

The downside of ANFIS prediction in study has been seen in the learning of the widely spaced data which existed in long distances. Improvement of the training algorithm of ANFIS using deep learning algorithms like PSO, deep NN and others is expected to further improve the mobility prediction.

References

[1] P. Cerwall, "Ericson mobility report," Stockholm, June 2015.

[2] P. Nisha, S. Shantanu and S. A. Kumar, "A survey on 5G: the next generation of mobile communication," *Physical Communication*, vol. 18, no. 2, p. 64–84, March 2016.

[3] P. Sharma, "Evolution of mobile wireless communication networks-1G to 5G as well as future prospective of next generation communication network," *International Journal of Computer Science and Mobile Computing*, vol. 2, no. 8, pp. 47-53, August 2013.

[4] M. Farooq, M. I. Ahmed and M. Usman, "Future generations of mobile communication networks," *Academy of Contemporary Research Journal*, vol. 2, no. 1, p. 24–30, 2013.

[5] S. Shukla, V. Khare, S. Garg and P. Sharma, "Comparative study of 1G, 2G, 3G and 4G," *Journal of Engineering, Computers & Applied Sciences (JEC&AS)*, vol. 2, no. 4, p. 55–63, April 2013.

[6] H. Wang, L. Ding, P. Wu, Z. Pan, N. Liu and X. You, "Dynamic load balancing and throughput optimization in 3GPP LTE networks," *Proceedings of the 6th International Wireless Communications and Mobile Computing Conference*, p. 939–943, 2010.

[7] B. Liang and Z. J. Haas, "Predictive distance-based mobility management for multidimensional PCS network," *IEEE/ACM Transactions on Networking*, vol. 11, no. 5, pp. 718-732, 2003.

[8] H. A. Karimi and X. Liu, "A predictive location model for location-based services," in *ACM-GIS 2003, Proceedings of the Eleventh ACM International Symposium on Advances in Geographic Information Systems*, New Orleans, Louisiana, USA, 2003.

[9] Z. R. Zaidi and B. L. Mark, "Real-time mobility tracking algorithms for cellular networks based on kalman filtering," *IEEE TRANSACTIONS ON MOBILE COMPUTING*, vol. 4, no. 2, pp. 195 - 208, 2005.

[10] S. Venkatachalaiah, R. J. Harris and R. Suryasaputra, "Improvement of handoff in wireless networks using mobility prediction and multicasting techniques," *Centre for Advanced Technology in Telecommunications (CATT)*, 2005.

[11] E. Kayacan, B. Ulutas and O. Kaynak, "Grey system theory-based models in time series prediction," *Expert Systems with Applications*, vol. 37, p. 1784–1789, 2010.

[12] J. L. Deng, "Introduction to Grey system theory," *The Journal of Grey System*, vol. 1, no. 1, pp. 1-24, 1989.

[13] E. A. Ubom, V. E. Idigo, A. O. C. Azubogu, C. O. Ohaneme and T. L. Alumona, "Path loss characterization of wireless propagation for south – south region of Nigeria," *International Journal of Computer Theory and Engineering*, vol. 3, no. 3, pp. 360-364, June 2011.

[14] N. V. Okorogu, U. D. Onyishi., C. G. Nwalozie and N. N. Utebor, "Empirical characterization of propagation path loss and performance evaluation for co-site urban environment," *International Journal of Computer Applications (0975 – 8887)*, vol. 70, no. 10, pp. 34 - 41, May 2013.

[15] O. S. Oguejiofor, V. N. Okorogu, A. Adewale and B. O. Osuesu, "Outdoor localization system using RSSI measurement of wireless sensor network," *International Journal of Innovative*

Technology and Exploring Engineering (IJITEE), vol. 2, no. 2, pp. 1 - 6, 2013.

[16] E. Ifeagwu, M. Alor and G. Obi, "Received signal strength estimation in wireless local area network (WLAN) Environment," *International Journal of Scientific Research in Science, Engineering and Technology* , vol. 1, no. 3, p. 183–186, 2015.

[17] S. Y. Seidel and T. Rappaport, "914 MHz Path loss prediction models for indoor wireless communications in multifloored building," *IEEE Transactions on Antennas and Propagation*, vol. 40, no. 2, p. 207–217, 1992.

[18] S. Zhaozheng, J. Qingzhe and J. Yanjun, "The combined model of Gray theory and neural network which is based on matlab software for forecasting of oil product demand," *Scientific Research*, p. 155–160, 2010.

[19] L. Xiaofei and H. Renfang, "Interpolation optimization interpolation optimization," *SHS Web of Conferences*, vol. 6, no. 03003, pp. 1-6, 2014.

[20] P. Zhou, B. W. Ang and K. L. Poh, "A trigonometric grey prediction approach to forecasting electricity energy demand," *Energy*, vol. 31, no. 14, pp. 2839-2847, 2006.

[21] Y. Chakrapani and K. Soundararajan, "Adaptive neuro-fuzzy inference system based fractal image compression," *International Journal of Recent Trends in Engineering and Technology*, vol. 1, no. 2, pp. 47-51, 2009.

[22] K. V. Rop, D. B. O. Konditi, H. A. Ouma and S. M. Musyoki, "Parameter optimization in design of a rectangular microstrip patch antenna using adaptive neuro-fuzzy inference system technique," *International Journal on Technical and Physical Problems of Engineering (IJTPE)*, vol. 4, no. 3, pp. 16-23.

[23] K. B. Ariffin, "On Neuro-fuzzy applications for automatic control, supervision, and fault diagnosis for water treatment plant," A Thesis submitted to the Faculty of Electrical Engineering, Universiti Teknologi, Malaysia, 2007.

[24] T. N. Kapetanakis, I. O. V. G. S. Liodakis and A. Maras, "Solving the inverse loop antenna radiation problem using a hybrid neuro-fuzzy system," *20th Telecommunications forum TELFOR 2012 Serbia, Belgrade*, p. 1189–1192, Nov. 2012.

[25] J. J. Cárdenas, A. García, J. L. Romeral and K. Kampouropoulos, "Evolutive ANFIS training for energy load profile forecast for an iems in an automated factory," *Emerging Technologies & Factory Automation (ETFA), 2011 IEEE 16th Conference on, Toulouse*, pp. 1-8, 2011.

[26] S. Sharma, U. Kalra, S. Srivathsan, K. Rana and V. Kumar, "Efficient air pollutants prediction using ANFIS trained by modified PSO algorithm," *Reliability, Infocom Technologies and Optimization (ICRITO) (Trends and Future Directions), 2015 4th International Conference on, Noida*, pp. 1-6, 2015.

[27] S. K. Gharghan, R. Nordin, M. Ismail and J. A. Ali, "Accurate wireless sensor localization technique based on hybrid PSO-ANN algorithm for indoor and outdoor track cycling," *IEEE Sensors Journal*, vol. 16, no. 2, pp. 529 - 541, Jan. 15, 2016.

[28] M. Bernas and B. Płaczek, "Fully connected neural networks ensemble with signal strength clustering for indoor localization in wireless sensor networks," *International Journal of Distributed Sensor Networks*, vol. 2015, pp. 1 - 10, 2015.

[29] A. Payal, C. S. Rai and B. V. R. Reddy, "Artificial neural networks for developing localization framework in wireless sensor networks," *in Proc IEEE Int. Conf. Data Mining Intell. Comput. (ICDMIC)*, pp. 1-6, ep. 2014.

[30] A. Payal, C. S. Rai and B. V. R. Reddy, "Comparative analysis of Bayesian regularization and Levenberg–Marquardt training algorithm for localization in wireless sensor network," *in Proc. IEEE 15th Int. Conf. Adv. Commun. Technol. (ICACT)*, pp. 192-194, Jan 2013.

[31] S. Kumar and S. R. Lee, "Localization with RSSI values for wireless sensor networks: an artificial neural network approach," *in Proc. 1st Int. Electron. Conf. Sensors Appl.*, pp. 1-6, Jan. 2014.

[32] P.-J. Chuang and Y.-J. Jiang, "Effective neural network-based node localisation scheme for wireless sensor networks," *IET Wireless Sensor Syst.*, vol. 4, no. 2, pp. 97-103, 2014.